

# Information Retrieval by Electrical Capacitance Tomography: Evaluation of an Iterative Algorithm and the Importance of Boundary Conditions

H McCann\*, W Q Yang\* and N P Polydorides†

Department of Electrical Engineering and Electronics, UMIST, P O Box 88, Manchester M60 1QD, UK, email McCann@fs5.ee.umist.ac.uk

\* HMcC and WQY are members of the Virtual Centre for Industrial Process Tomography

† Now with the University of Oxford

**Abstract** – Empirical performance of a newly developed iterative image reconstruction algorithm for electrical capacitance tomography (ECT) has been assessed by the use of various phantoms. It is based on the retrieval of information relating to the gross features of each phantom, rather than  $\epsilon_r$  of each individual pixel. Some practical limitations of the present algorithm have been identified. It has been found experimentally that the number of independent information elements retrieved approaches the number of independent capacitance measurements. Analysis of electrostatic boundary conditions for ECT is also presented, indicating a large number of physical constraints for image reconstruction, in addition to the capacitance measurements. It is suggested that the iterative algorithm carries out implicit regularisation with those constraints, and that the information content of ECT images could be much larger than previously suggested. An alternative measurement protocol is proposed to enhance further the information content.

**Keywords:** Capacitance tomography, Iterative image reconstruction, Experiment evaluation

## 1. INTRODUCTION

### 1.1 The problem

A distinguishing feature of electrical tomography is that, in principle, the whole imaging space can contribute to every electrical signal measured at the periphery. This is due to the “soft-field” nature of the technique, in that the electric field lines are distorted everywhere by non-homogeneity of electrical properties in the subject [1].

In this paper, electrical capacitance tomography (ECT) is considered, which is illustrated schematically in Figure 1. The system obtains  $M$  distinct measurements of the charges  $Q_{ij}$  induced on sensing electrode  $j$  when source electrode  $i$  is energised. In the conventional approach, one electrode is excited and all the others are used to measure charge and the maximum value of  $M$  is  $N(N-1)/2$ .

As discussed by [2],  $Q_{ij}$  is given via Gauss’s law

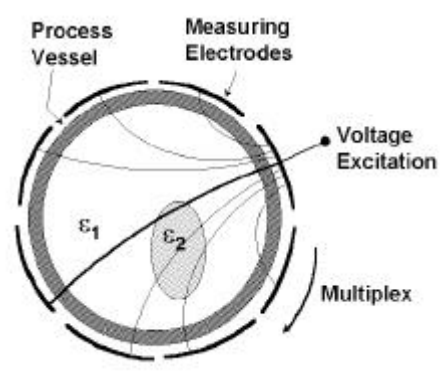


Figure 1 N-electrode ECT sensor, showing a schematic representation of electric field lines

$$Q_{ij} = \iint_A \epsilon(x, y) \vec{E} d\vec{A} \quad (1)$$

where  $\epsilon(x, y)$  is the permittivity distribution,  $\vec{E}$  is the electric field, and  $A$  is the integration surface enclosing electrode  $j$ .

The potential distribution  $V(x, y)$  is given by

$$\nabla^2 V(x, y) + \frac{1}{\epsilon(x, y)} \nabla V \cdot \nabla \epsilon(x, y) = 0$$

(2)

The objective of ECT is to determine  $\varepsilon(x, y)$  from measurements of  $Q_{ij}$ . However, equation (1) implies a requirement to know  $\vec{E}$  at every point on the integration surface  $A$ , whilst equation (2) demonstrates that  $\vec{E} = -\nabla V(x, y)$  can not be obtained without knowledge of  $\varepsilon(x, y)$ . This non-linear coupling is the main problem of image reconstruction for ECT. Moreover, as discussed by [3], the inversion of equations (1) and (2) is ill-posed, and the  $\varepsilon(x, y)$  solution may not be unique, may not exist for some given  $Q_{ij}$  data, or may not depend continuously on the data. Regularisation of the solution by using additional physical information can therefore be of critical importance, e.g.  $\varepsilon(x, y) > 0$ .

## 1.2 Image reconstruction

This inversion problem has been studied in various linearised forms from a variety of angles as discussed and reviewed in [1, 2, 5]. A popular approach is linear back projection (LBP), where a sensitivity matrix  $\mathbf{S}$  is defined to relate the measured capacitance  $C_{ij}$  to the permittivity of each pixel  $k$ ,  $\varepsilon_k$ , in the image *via* the relationship [4]

$$C_{ij} = \sum_{k=1}^K S_{ijk} \varepsilon_k \quad (3)$$

where  $K$  is the total number of pixels in the image.

In principle, the image is obtained by inverting this equation. In practice, the inverse of  $\mathbf{S}$  does not exist.  $K$  is normally defined arbitrarily. Clearly, the larger  $K$  is, in relation to  $M$ , the less determined are the individual  $\varepsilon_k$ . Typically,  $K$  is much larger than  $M$ , considerably increasing the degree of ill-posedness of the inversion. For any given application, evaluation of the robustness of  $\varepsilon(x, y)$  images, against a range of experimental parameters, is essential. Therefore, it is important to ensure that the range of  $\varepsilon(x, y)$  solutions to the inversion process is acceptable for a particular application. In most cases, the user is concerned to ensure the performance of the system in terms of how it reproduces the gross features of the object under study, and is less concerned about the accuracy of each pixel value  $\varepsilon_k$ .

Various attempts have been made to reconstruct  $\varepsilon(x, y)$  images by iterative and/or non-linear techniques [4, 5, 7]. The iterative methods appear to have considerable promise, albeit at the expense of more complex algorithms and significant computational power.

We focus here on the performance of the algorithm in [4]. Although this algorithm is still open to further improvement, its present performance has been demonstrated experimentally. The aim of the experimental work is to determine the maximum number,  $I_{\max}$ , of independent information elements (IIE) describing the gross features of an object, which could be retrieved from a set of measured data by this technique. Note that IIE is a property of the phantom and  $I_{\max}$  is the result of reconstruction. The experimental results have stimulated further analysis of the problem.

## 2. EXPERIMENTAL PROCEDURE

An 8-electrode ECT system (i.e.  $N = 8$ ) was used, which incorporated recent advances in analogue sensitivity with AC excitation [8]. In this system the maximum number of independent capacitance measurements is  $M = N(N-1)/2 = 28$ . A series of phantoms, of varying complexity, were constructed from cylindrical and rectangular rods of different sizes and different permittivities, the host medium being air. Each phantom was represented by a set of information parameters, comprising:

- the location of its centre ( $x_C, y_C$ );
- its geometrical properties (radius for a cylindrical object; length of its sides for a rectangular object);
- its orientation (in the case of a rectangular object);
- its permittivity  $\varepsilon_r$ .

Hence, a cylindrical object presents 4 IIEs, and a rectangular one 6. When several such objects are included within a single complex phantom, a large number of IIEs can be found in the overall phantom.

Rods of two different materials were used: ultra-high molecular weight polyethylene (PE) of permittivity,  $\varepsilon_r = 2.3$ ; and glass-filled polyester material (GRP) of  $\varepsilon_r = 4.0$  (at 1 MHz). The ECT sensor was aligned vertically on a base plate with a grid of fixing holes used to secure the rods in position. For the purposes of illustration, Figure 2 (a) shows a plan view of an arrangement of 3 rods, 2 cylindrical and 1 rectangular, which can be described by 14 IIEs.

Data were measured as described in [8] and reconstructed by the iterative algorithm described in [4], with a set of finite element field solutions in each iteration step. Figure 2 (b) shows the reconstructed image of the phantom.

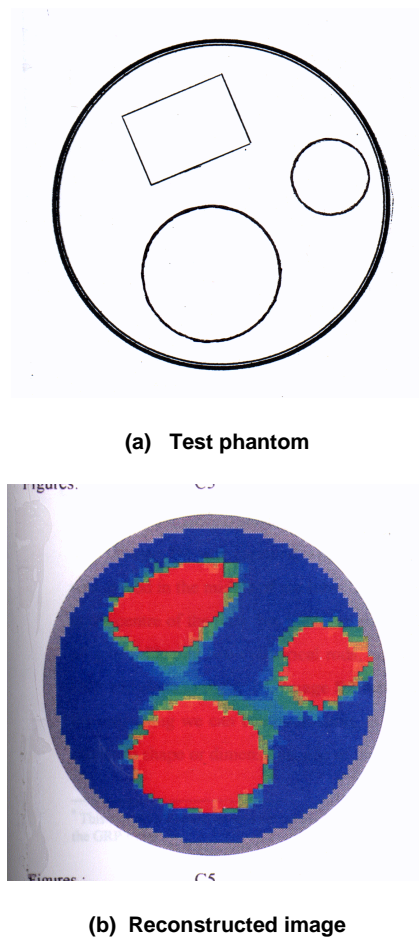


Figure 2 Reconstruction of a phantom consisting of 3 rods

### 3. EXPERIMENTAL RESULTS

#### 3.1 Restrictions on phantom complexity

For a fixed diameter ECT sensor (84 mm), insertion of a large number of rods entails a reduction in the size of the rods and/or that the boundaries of the rods are close together, and/or that the boundaries of the objects are close to the sensor perimeter. In the first case, the combined analogue measurement sensitivity and spatial resolution of the system were found to be severely challenged. Rods of cross sectional area about 8% of the total sensor cross-sectional area or less, were difficult to reproduce faithfully.

In the second case, the requirements on spatial resolution were found to be extremely demanding; rods which were placed less than 7 or 8 mm apart were “merged together” in the images, preventing their separate shape identification. When rods were placed close to the wall, some distortions occurred in the area near the wall, but their shape could be distinguished if they were large enough. By such studies, a procedure was developed to avoid the worst aspects of the above constraints.

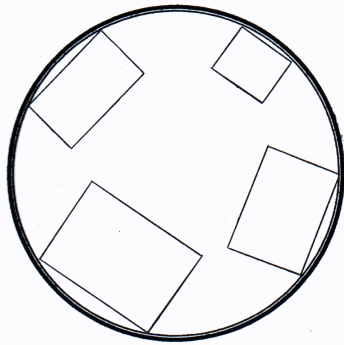
Difficulties were also encountered when rods of different  $\epsilon_r$  were used within a single phantom because the present calibration procedure requires the use of the highest  $\epsilon_r$  material and air only. It has been found that the reconstruction of complex phantoms does not reliably reproduce intermediate values of dielectric constant. Even when a single rod of a lower  $\epsilon_r$  is used in the test phantom, prior calibration by the use of the higher  $\epsilon_r$  material forces the reconstruction of the test phantom to have some small regions of maximum  $\epsilon_r$ . This is due to the fact that the present algorithm is based on two distinct components, rather than continuous permittivities.

In favourable cases, it has been found that at least 21 IIEs can be retrieved by the ECT system. Figure 3 shows an example: 4 rectangular PE rods are very well reconstructed. Since the reconstruction of dielectric constant has been shown to be unreliable, the number of IIE retrieved is  $(4 \times 6) - 3 = 21$ . The various procedural problems noted above suggest that, with feasible improvements in experimental procedure and in the reconstruction software (such as freedom to set  $\epsilon_r$  between 1 and  $\epsilon_{rmax}$ ), a larger number of IIE may be retrieved.

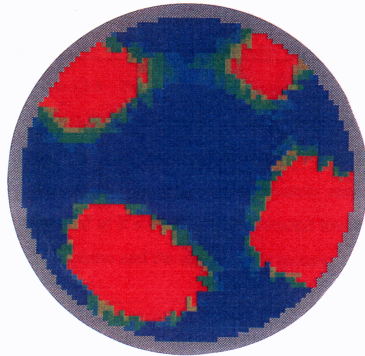
### 4. DISCUSSION

#### 4.1 $I_{max}$

As noted in Section 1, many previous authors [1, 2, 5] have studied linearised approaches to the image reconstruction problem in ECT. It is implicit in these approaches that, without any form of regularisation, the upper limit of  $I_{max}$  is  $M$ , i.e. 28 in the present case. Several authors (e.g. [6]) have asserted that not all of the  $C_{ij}$  are independent, hence  $I_{max}$  will generally be less than  $M$ . The data presented here show that, even for very simple  $\epsilon_r$  distributions, the experimentally achievable value of  $I_{max}$  approaches  $M$ . Furthermore, the various problems noted in Section 3 regarding experimental and simple algorithmic limitations, indicate the promise that the relationship  $I_{max} = M$  can be breached by the methods developed in [4].



(a) Test phantom



(b) Reconstructed image

Figure 3 Reconstruction of a phantom consisting of 4 rods

#### 4.2 Constraints

The measurement protocol imposes implicit constraints on the reconstruction process due to the electrostatic boundary conditions. The iterative technique [4] solves the electrostatic field equations at each step in the iteration process. Therefore, the inclusion of such a step in an iterative process amounts to an implicit regularisation method [3].

At each electrode, the following boundary conditions apply, from electrostatics [9]:

- (a) the normal component of the displacement field  $D_n$  must be equal to the surface density of the free charges,  $D_n = \mathbf{e}_o \mathbf{e}_r E_n = \mathbf{S}_r$ ;
- (b) the tangential component of the electric field in the object, adjacent to the surface of each electrode, must be zero;
- (c) the voltage at infinity is zero;
- (d) the voltage varies continuously across the interface from any electrode to the material of the object.

The only part of the above set of boundary conditions which is explicitly taken into account in the LBP reconstruction process is part (a), i.e. the

measurements of  $Q_{ij}$ . Therefore, boundary condition (a) yields  $N(N-1)/2$  parameters to be used in the reconstruction process. All of the other boundary conditions (b) - (d) offer the possibility to improve the reconstruction by regularisation [3], either by explicit inclusion in the inversion process or by post-reconstruction inclusion.

It is suggested that (b) and (c) each offer at least  $N$  additional constraints in the whole process (one per excitation) and (d) offers one per electrode per excitation, i.e. at least  $N(N-1)/2$ . Therefore,  $I_{max}$  is at least 72 for  $N = 8$ , rather than 28.

#### 4.3 Implications

Using the above simple electrostatic analysis, we suggest that, in principle,  $I_{max}$  is significantly larger than  $M$ : at least  $2N(N-1)/2 + 2N = N(N+1)$ . If the electrostatic analysis holds, it is clear that the present measurement protocol is degenerate, because the sensing electrodes are always held at identical and constant potentials. There is a possibility of further increasing the information content of ECT by active manipulation of the boundary conditions, e.g. by setting the potentials of the individual measurement electrodes at different levels for each individual excitation or detection configuration. In physical terms, this can be explained as follows:

- The currently degenerate protocol imposes a set of  $N$  grossly different electric field configurations, with each electrode in turn acting as the source of electric flux lines;
- The potentials of the measurement electrodes, as well as the distribution of  $\epsilon_r$ , influence the local electric field lines and hence  $Q_{ij}$ ;
- If, for each major field excitation case, the potential of each individual measurement electrode,  $V_{mj}$  is varied, then additional measurements of  $Q_{ij}(V_{mj})$  may be made. Clearly, the hardware measurement sensitivity to changes in  $Q_{ij}(V_{mj})$  will determine the practical extent to which this approach can be exploited.

This last case corresponds to a case where the electric field lines through the object are varied through many more intermediate configurations than is the case in the present protocol.

#### 5. CONCLUSIONS

It has been shown that improvements remain to be implemented in the iterative reconstruction technique of [4]. However, the performance of that technique is encouraging. A new approach

has been defined to assess information retrieval performance by ECT, based on the gross features of the object, rather than the values of individual image pixels. This offers simple ways to assess system performance.

The maximum number of IIE which can be retrieved by ECT, is shown experimentally to approach  $M = N(N-1)/2$ , and may exceed  $M$  if some improvements both to the iterative reconstruction algorithm and the experimental (calibration) procedure can be implemented.

A simple electrostatic analysis of boundary conditions suggests that the above satisfactory performance is due to implicit regularisation of the LBP process by carrying out field solution in the new iterative process. A new electrostatic analysis suggests that the information content of ECT may be increased by active manipulation of boundary conditions in the measurement protocol, provided that the charge measurement hardware is sufficiently sensitive.

## REFERENCES

- [1] R.A.Williams and M.S.Beck, (Eds.), "Process Tomography: Principles, Techniques and Applications", Butterworth-Heinemann, Oxford, 1995
- [2] N.Reinecke and D.Mewes, "Recent developments and industrial/research applications of capacitance tomography", *Meas. Sci. Technol.*, 1996, **7**, pp 223-246.
- [3] M.Bertero and P.Boccacci, "Introduction to Inverse Problems in Imaging", Institute of Physics Publishing, Bristol, 1998
- [4] W.Q.Yang, D.M.Spink, T.A.York and H.McCann, "An iterative reconstruction algorithm based on the Landweber iteration method for capacitance tomography", *IEEE Trans. Image Processing* (submitted)
- [5] O.Isaksen, "A review of reconstruction techniques for capacitance tomography", *Meas. Sci. Technol.*, 1996, **7**, pp 325-327.
- [6] F.T.Kuhn, J.C.Schouten, C.M. van den Beek and B.Scarlett, B, "A least squares image reconstruction algorithm for Electrical Capacitance Tomography", *Proc. Frontiers in Industrial Process Tomography II*, Delft, Netherlands, (Publ. Engineering Foundation, New York), 1997, pp 189-194
- [7] A.Trachtler, "A fast non-linear reconstruction technique for Electrical Impedance Tomography", *Proc. Frontiers in Industrial Process Tomography II*, Delft, Netherlands, (Publ. Engineering Foundation, New York), 1997, pp 211-217
- [8] W.Q.Yang and T.A.York, "New AC-based capacitance tomography system", *IEE Proc.-Sci. Meas. Techn.*, **146**, 1999 (in press)
- [9] P.Lorrain and D.Corson, "Electromagnetic Fields and Waves", W.H.Freeman & Co., San Francisco, 1970